28. Shackleton, N. J., Berger, A. & Peltier, W. R. An alternative astronomical calibration of the lower Pleistocene timescale based on ODP site 677. *Trans. R. Soc. Edinb. Earth Sci.* **81,** 251–261 (1990).
29. Maasch, K. A. Statistical detection of the mid-Pleistocene transition. *Clim. Dyn.* **2,** 133–143 (1988).
30. Chambers, J., Cleveland, W., Kleiner, B. & Tukey, P. *Graphical Methods for Data Analysis* 395 (Chapman & Hall/CRC, Boca Raton, 1983).

Supplementary information is available on *Nature*'s World-Wide Web site (http://www.nature.com) or as paper copy from the London editorial office of *Nature*.

Acknowledgements

We thank the BDP Leg IV members from Russia, America and Japan who worked to drill the BDP98 sediment cores, and J. Laskar, A. Berger and M.-F. Loutre for providing the calculated results on insolation. We also thank colleagues in the hydro-geomorphological laboratory at Kanazawa University and the geomagnetic laboratory of Toyama University for their support in this research.

Correspondence and requests for materials should be addressed to K.K. (e-mail: kashi@kenroku.kanazawa-u.ac.jp).

Earthquake slip on oceanic transform faults

Rachel E. Abercrombie & Göran Ekström

Department of Earth and Planetary Sciences, Harvard University, 20 Oxford Street, Cambridge, Massachusetts 02138, USA

Oceanic transform faults are one of the main types of plate boundary, but the manner in which they slip remains poorly understood. Early studies suggested that relatively slow earthquake rupture might be common[1,2]; moreover, it has been reported that very slow slip precedes some oceanic transform earthquakes, including the 1994 Romanche earthquake[3–5]. The presence of such detectable precursors would have obvious implications for earthquake prediction. Here we model broadband seismograms of body waves to obtain well-resolved depths and rupture mechanisms for 14 earthquakes on the Romanche and Chain transform faults in the equatorial Atlantic Ocean. We found that earthquakes on the longer Romanche transform are systematically deeper than those on the neighbouring Chain transform. These depths indicate that the maximum depth of brittle failure is at a temperature of ~600 °C in oceanic lithosphere. We find that the body waves from the Romanche 1994 earthquake can be well modelled with relatively deep slip on a single fault, and we use the mechanism and depth of this earthquake to recalculate its source spectrum. The previously reported slow precursor can be explained as an artefact of uncertainties in the assumed model parameters.

The depth extent of seismic slip in shallow oceanic earthquakes is poorly known, limiting our understanding of how oceanic transform faults move, and how the lithospheric composition affects the earthquake rupture process. Estimates of seismic coupling determined from the ratio of seismic slip to plate motion by summing the earthquake moments are crucially dependent on the width of the fault assumed to slip in earthquakes. Oceanic crust is only ~6 km thick. Theoretical strength profiles predict that seismic slip should extend into the upper mantle, unlike continents, where it is restricted to the upper crust[6].

The international agencies locating earthquakes typically report the depth of earthquakes on oceanic ridges and transforms as 10 or 15 km. More accurate depths and mechanisms of oceanic earthquakes have been obtained by modelling long period (LP) body waves[7–9]. The depths of oceanic intraplate earthquakes increase with lithospheric age, implying that temperature controls the depth of the brittle–ductile transition[7]. The LP data were inadequate to resolve similar trends in the depths of earthquakes along the relatively young transform faults. Few transform fault studies have used ocean-bottom seismometers, and most were unable to resolve hypocentres accurately[10].

Very slow slip occurs in some earthquakes[11], but the observations of oceanic transform earthquakes[3–5] remain controversial. This is because the hypothesized slow component is often a small fraction of the total moment and because other authors have failed to confirm the proposed slow rupture during the largest earthquake considered[12,13]. The shape of the long-period spectrum, used to identify possible slow rupture, is strongly dependent on the Earth structure and source parameters (including depth) assumed in the modelling[14]. More accurate measurements of these parameters are therefore necessary.

Modern broadband data have significantly higher resolution than the LP data. We use these data to compare earthquakes on two contrasting transform faults on the equatorial Mid-Atlantic Ridge.

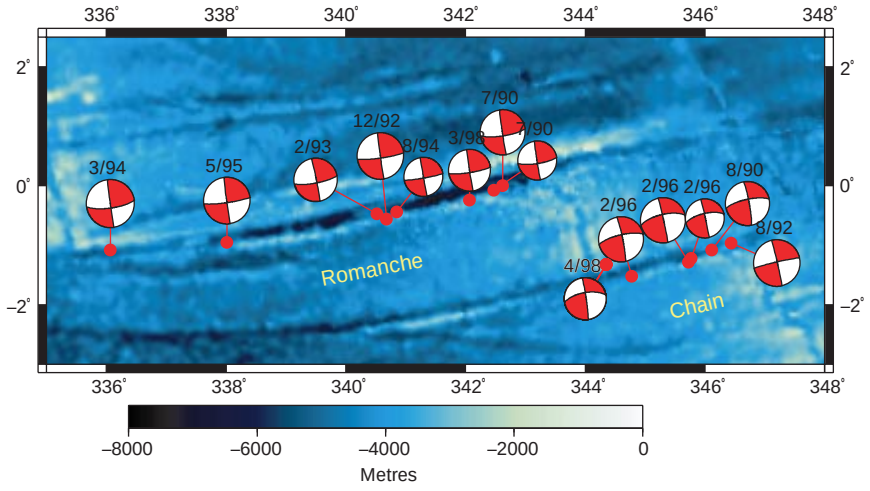

Figure 1 Map of the equatorial Mid-Atlantic Ridge, showing the Romanche and Chain transform faults and also the bathymetry[26,27]. The transform valleys are dark blue and the interconnecting ridges are pale blue. The focal mechanisms obtained in the broadband body-wave modelling are joined to their National Earthquake Information Center hypocentre locations (red circles), with radius proportional to magnitude. The earthquakes on the Romanche transform all dip to the south at ~80°, and those on the Chain transform all dip to the north at ~73°. The centroid-moment tensor (CMT) mechanisms are not accurate enough to resolve these differences. The active faults thus seem planar, but the reason for their opposite sense of dip is unknown.

We compare earthquakes on the Romanche transform, which is one of the longest on the mid-ocean ridge system and offsets 50-Myr lithosphere, with events on the neighbouring Chain transform, which is shorter and offsets younger lithosphere (17 Myr) (Fig. 1). We use broadband body waves to determine focal mechanisms and depths for the 14 largest earthquakes in the Harvard CMT catalogue since 1990 (refs 15, 16) (Figs 1 and 2). Most of these earthquakes are well recorded, and depths and mechanisms are well constrained.

The mechanisms of the earthquakes on each transform are extremely similar. They all have strikes within 2° of the strike of the transforms (~80°), implying that the transform faults are planar. Using these well-constrained focal mechanisms, we determine the distribution of slip in the largest, 1994 Romanche, earthquake (Fig. 3). This earthquake has previously been reported to have a complex rupture, including a slow precursor[4]. Strong eastward directivity is clear in the waveforms. The earthquake had a small amplitude onset lasting about 12 s (subevent A (ref. 4), which is not unusual for a large earthquake[17]. The main slip occurred in two large subevents to the east of the hypocentre. Their centroid depth agrees well with that obtained from the body-wave modelling (12 km; all depths quoted are below the sea floor) and seismic slip extends to

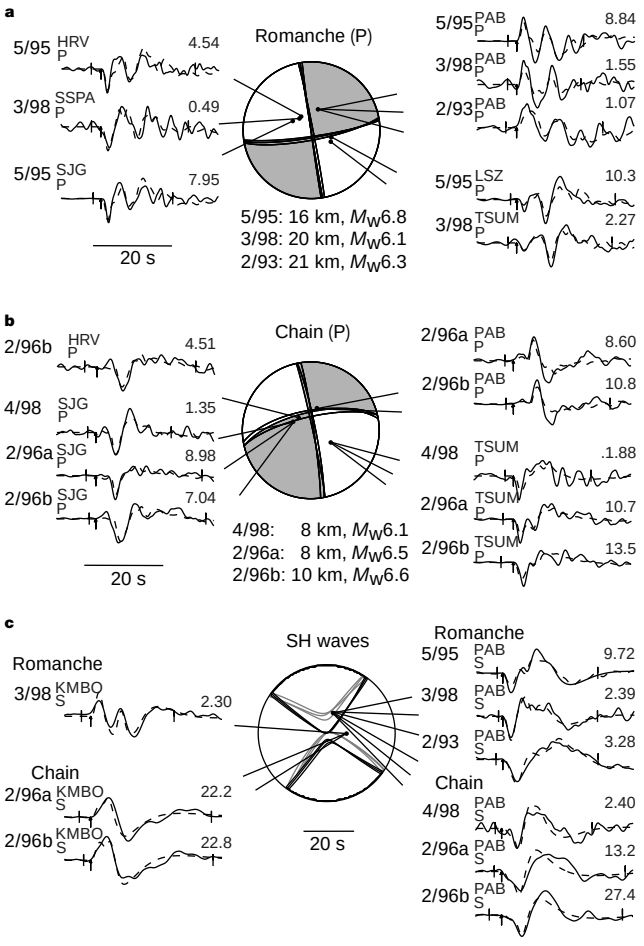

Figure 2 Comparison of the waveforms from six earthquakes, three on each of the Romanche and Chain transforms. The observed displacement broadband waveforms (solid lines, 20 samples per second), are corrected for the instrument response and filtered between 1 and 150 s. The dashed lines are the synthetics. The stations are chosen to allow comparison between earthquakes on each transform and between transforms. The dates, depths and magnitudes are given. The amplitudes of the seismograms (μm) are given at the top right. The arrows mark the P picks; the vertical lines indicate the duration used in the inversion. **a**, **b**, P waves are shown from earthquakes on the Romanche transform (**a**) and the Chain transform (**b**). All six mechanisms are shown, and those of the 1995 and February 1996b earthquakes are shaded. **c**, SH waves from all six earthquakes. The SH mechanisms of the Romanche earthquakes are shown in black, and those on Chain in grey. The seismograms from earthquakes on individual transforms are very similar but differ between transforms, constraining the different dip directions. The depths of the earthquakes are well constrained by the arrival times of the depth phases. The waveforms of the Chain earthquakes are shorter in duration than the Romanche events, implying that they are shallower. P wave arrival times are picked on velocity seismograms. The P and SH waveforms (between 9 and 36 per earthquake) are inverted for mechanism, centroid depth and moment rate[28]. The model source structure consists of 5 km of water above a 6-km crust[28]. Non-double couple components were initially included but were negligible, and the mechanisms are fixed to double couples. Rupture velocity is included when it significantly improves the fit. The data for two earthquakes (July 1990c, Fig. 1, and February 1996b) are insufficient to constrain the mechanisms and so they are set equal to those of neighbouring events with similar waveforms.

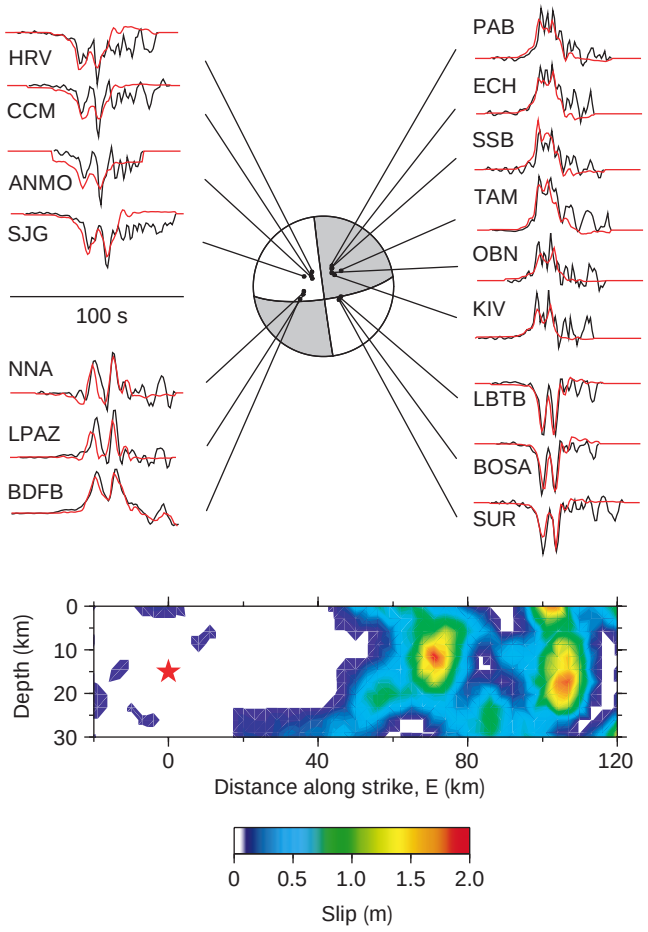

Figure 3 Inversion for slip distribution in the 14 March 1994 Romanche earthquake (M_W 7.1). We use the mechanism obtained in the body-wave modelling (strike 82°, dip 75°, rake 179°) to invert for slip on a finite fault plane. We use broadband displacement P waves, low-pass-filtered at 1 Hz. We use an oceanic structure and invert for slip on a 150 km × 39 km fault plane divided into 3 km × 3 km subfaults, extending from the sea floor (0 km)[29]. We use fixed rupture velocities between 3.0 and 4.5 km s^{-1}, but only those between 3.5 and 4 km s^{-1} can fit the waveforms well. The observed waveforms are shown in black (labelled with station code) and the synthetics in red. The strong eastward directivity is clear when the arrival times of the first large pulse and the duration of the waveforms in the east are compared with those in the west. All the synthetic seismograms start 20 s before the predicted arrival time. The preferred model is for a rupture velocity of 4 km s^{-1}, and has a moment of 5.1×10^{19} N m. Two large subevents are well resolved, and some small slip occurred near the hypocentre. The depth range is from near the surface to ~20 km. Slip in the upper 5 km, and below 20 km, is not required; constraining the slip to between these depths results in an insignificant decrease in fit. The variance decrease of the preferred model is 80%.

~20 km. The first of these subevents corresponds to subevent B (ref. 4). McGuire *et al.*[4] identified subevents by picking arrivals in the observed seismograms; they did no waveform modelling. This is difficult for strike-slip earthquakes in which many arrivals are small or nodal. From the timing of their picks, McGuire *et al.* located subevent B 80 km northeast of A, on a separate fault. This jump is over an order of magnitude greater than observed in surface ruptures[18] or numerical simulations[19]. Our model does not need such a jump, and requiring it worsens the waveform fit. In our mechanism the stations to the SE are nodal, and those to the SW have small P amplitudes (Fig. 3). We infer that McGuire *et al.*[4] misidentified the strong surface reflections (such as sP) as P. This would result in an overestimate of the time delay between the two subevents at the southern stations and would thus displace the location of subevent B to the north. Waveform modelling in the frequency range in which most energy is radiated is essential when investigating strike-slip earthquakes.

McGuire *et al.*[4] also modelled the long-period source spectrum of the 1994 Romanche earthquake. They used synthetic reference seismograms calculated for an earthquake located in the 21-km crust in the Preliminary Reference Earth Model (PREM)[20] at a fixed depth of 15 km to obtain the source spectrum (Fig. 4). We recalculate the source spectrum using an oceanic crustal model at the source, and determine the mechanism and depth independently from the body-wave modelling. The resulting spectrum is flat at long periods with no resolvable slow component (Fig. 4). The recalculated source spectrum is in good agreement with the source spectrum predicted in the slip inversion of the higher-frequency body waves. This suggests that the proposed slow component is an artefact of using an inadequate source model. A small precursory ramp in the highly filtered time-domain records has also been claimed as supporting evidence for precursory slip[4], but the amplitude is so small that these observations are ambiguous.

The depths of all 14 earthquakes obtained in the broadband body-wave modelling are shown in Fig. 5. The systematic difference between the two transforms is clear. The earthquakes on Romanche have centroid depths between 7 and 20 km, and those on Chain between 3 and 11 km. The Romanche transform offsets relatively old, cold lithosphere, and the systematic difference implies that temperature controls the maximum depth of seismic slip on oceanic transform faults as it does elsewhere[6,7]. The centroids are located in a similar temperature range on both transforms. We can estimate the rupture area of the earthquakes from slip inversions (Figs 3 and 5) and from global relationships between earthquake moment and rupture area[21]. The 600 °C isotherm thus seems a good estimate of the limit of seismic slip. This is consistent with previous results for intraplate oceanic earthquakes[7] but is cooler than previously estimated for transform fault events[9]. The depth of the isotherms can be

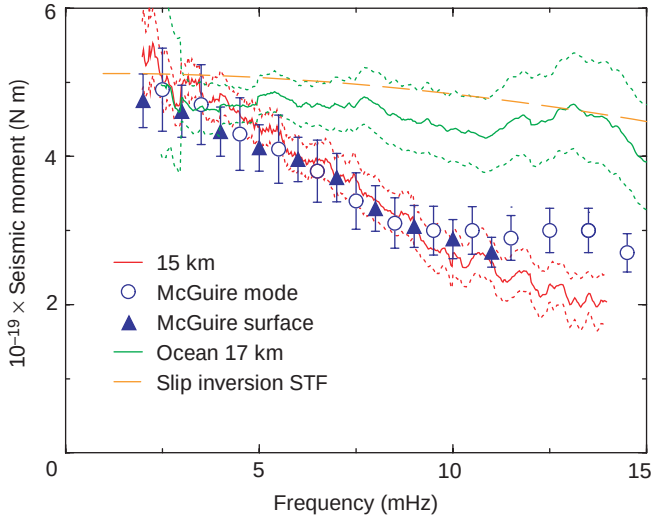

Figure 4 Long-period source spectra of the 1994 Romanche transform earthquake (M_w 7.0). The blue symbols are the spectrum obtained by McGuire *et al.*[4] from vertical Rayleigh waves by using the PREM[20] structure at the source, the Harvard CMT mechanism, and a depth of 15 km below the surface of the model. Note the increase in amplitude at frequencies below ~8 mHz, where the spectrum of a typical earthquake of this magnitude should be almost flat. It is this apparent excess long-period energy that is taken as evidence for a slow rupture component[3–5]. We obtain the source spectrum in a similar way, also using vertical Rayleigh waves. We calculate the synthetic seismograms with a hybrid method. Fundamental mode surface waves are synthesized with the use of WKBJ ray-theory, incorporating the excitation in an oceanic elastic structure. Overtones are calculated with normal-mode summation. The spectrum of the observed seismogram is divided by that of the synthetic at each station, and then all the stations are averaged to obtain the mean source spectrum. The red spectrum used synthetics calculated for 15 km depth in PREM[20] crustal structure and the Harvard catalogue CMT mechanism. The dotted lines are the 95% confidence limits of the mean. The results agree with those of McGuire *et al.*[4]. The green source spectrum is calculated using the mechanism and depth determined independently from the body waves (Fig. 3), and a more appropriate oceanic velocity structure at the source (5 km of water above a 6.5 km oceanic crust and PREM[20] mantle). The orange dashed line is the spectrum of the source time function (STF, 33 s duration) obtained from the slip inversion. The recalculated source spectrum (green) is consistent with that from the higher-frequency body waves, and shows no evidence of an increase in amplitude at long periods.

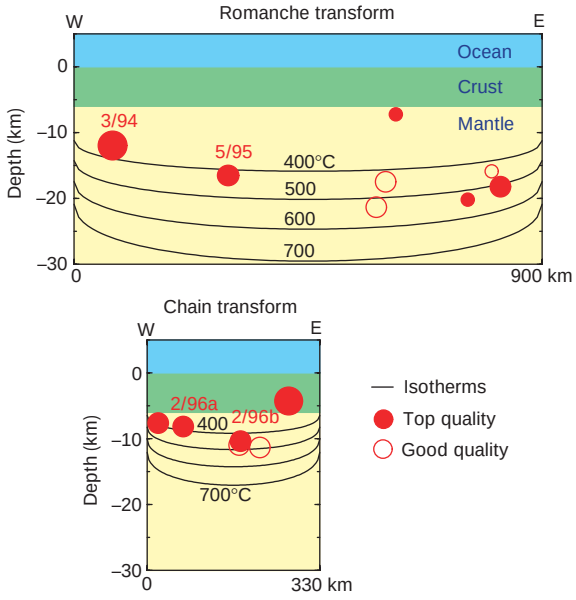

Figure 5 Depth and temperature of earthquakes on the Romanche and Chain transforms. The thickness of oceanic crust is about one-sixth that of average continental crust. The centroid depths of the earthquakes studied are plotted as red circles with symbol size proportional to magnitude. Solid symbols represent earthquakes with the best-resolved parameters, and open symbols those with fewer data or poorer fits. All the depths are accurate to within ~3 km. Isotherms, calculated by using a half-space cooling model and averaging both sides of the transform, are plotted in black[30]. Slip inversions of the 1994 and 1995 Romanche earthquakes suggest that the former ruptured from near the surface to ~20 km depth, and the latter from ~10 to 25 km depth. The 600 °C isotherm therefore seems a reasonable estimate of the temperature controlling the maximum depth of seismic slip on these transforms. The 1992 Chain earthquake is the only event with a centroid within the crust, but it was large enough to have ruptured into the upper mantle. We sum the moments of all the predominantly strike-slip earthquakes in the 25-yr Harvard CMT catalogue along the Romanche and Chain transforms. Assuming a rigidity of 3×10^{10} N m^{-2}, and assuming that the transforms have lengths of 900 and 330 km and widths of 20 and 13 km, respectively, we obtain a seismic slip rate of 17 mm yr^{-1} on Romanche and 20 mm yr^{-1} on Chain. The seismic slip during this period might not be representative of the longer-term average, but it is higher than that calculated for the Romanche transform by Brune[24] for the period 1920–52.

varied by using different thermal models[22]. The depths of the earthquakes depend on the assumed crustal thickness and velocities in the upper lithosphere, but reasonable variation[23] would make a difference of no more than 1 km. A temperature of 600 °C is approximate but is consistent with the onset of ductile deformation in olivine-rich materials at probable strain rates[7]. The systematic difference between the two transforms is independent of these uncertainties. The depths of the earthquakes on the Romanche transform are deeper than previously determined for oceanic transform earthquakes; they are also in older lithosphere.

The degree of seismic coupling of oceanic transform faults has remained poorly constrained since it was first studied[24], because the width of the seismic zone was unknown. Our large seismic widths result in relatively low seismic slip rates (Fig. 5), only about half of the 37 mm yr^{-1} tectonic slip rate[25].

If we are not underestimating the seismic slip, then half of the slip must be occurring aseismically. It has been suggested that aseismic and slow (possibly precursory) slip might occur in the upper mantle, whereas higher speed seismic slip occurs in a very shallow seismogenic zone[4]. The depth extent of the seismic slip in the 1994 and 1995 earthquakes (Figs 3 and 5) and the centroid depths of the other events provide clear evidence of seismic rupture extending well into the upper mantle. Our results imply that significant aseismic slip is occurring and it is likely to be at shallow depths, perhaps within the serpentinized zone.

The depth of seismic slip on oceanic transform faults is controlled by temperature and is limited by the ~600 °C isotherm. The focal mechanisms of earthquakes of the two transform faults show impressive consistency, indicating that the faults are highly planar. We also find that the two previously identified[4] unusual aspects of the 1994 Romanche earthquake are probably artefacts of the analysis procedure used. No detectable precursors to oceanic transform earthquakes can be resolved unambiguously with present seismic data and analysis techniques. □

Received 1 March; accepted 11 December 2000.

1. Kanamori, H. & Stewart, G. S. Mode of the strain release along the Gibbs fracture zone, Mid-Atlantic Ridge. *Phys. Earth Planet. Inter.* **11,** 312–332 (1976).
2. Okal, E. A. & Stewart, L. M. Slow earthquakes along oceanic fracture zones: evidence for asthenospheric flow away from hotspots? *Earth Planet. Sci. Lett.* **57,** 75–87 (1992).
3. Ihmlé, P. F. & Jordan, T. M. Teleseismic search for slow precursors to large earthquakes. *Science* **266,** 1547–1551 (1994).
4. McGuire, J. J., Ihmlé, P. F. & Jordan, T. H. Time domain observations of a slow precursor to the 1994 Romanche transform earthquake. *Science* **274,** 82–85 (1996).
5. Ihmlé, P. F., Harabaglia, P. & Jordan, T. H. Teleseismic detection of a slow precursor to the great 1989 Macquarie Ridge earthquake. *Science* **261,** 177–183 (1993).
6. Sibson, R. H. Fault zone models, heat flow and the depth distribution of earthquakes in the continental crust of the United States. *Bull. Seismol. Soc. Am.* **72,** 151–163 (1982).
7. Wiens, D. A. & Stein, S. Age dependence of oceanic intraplate seismicity and implications for lithospheric evolution. *J. Geophys. Res.* **88,** 6455–6468 (1983).
8. Engeln, J. F., Wiens, D. A. & Stein, S. Mechanisms and depths of Atlantic transform faults. *J. Geophys. Res.* **91,** 548–577 (1986).
9. Bergman, E. A. & Solomon, S. C. Transform fault earthquakes in the North Atlantic: source mechanisms and depth of faulting. *J. Geophys. Res.* **93,** 9027–9057 (1988).
10. Wilcock, W. S. D., Purdy, G. M. & Solomon, S. C. Microearthquake evidence for extensions across the Kane transform fault. *J. Geophys. Res.* **95,** 15439–15462 (1990).
11. Kanamori, H. & Kikuchi, M. The 1992 Nicaragua earthquake: a slow tsunami earthquake associated with subducted sediments. *Nature* **361,** 714–716 (1993).
12. Kedar, S., Watada, S. & Tanimoto, T. The 1989 Macquarie Ridge earthquake: seismic moment estimation from long period free oscillations. *J. Geophys. Res.* **99,** 17893–17907 (1994).
13. Velasco, A. A., Ammon, C. J. & Lay, T. Source time function complexity of the great 1989 Macquarie Ridge earthquake. *J. Geophys. Res.* **100,** 3989–4009 (1995).
14. Silver, P. G. & Jordan, T. H. Total-moment spectra of fourteen large earthquakes. *J. Geophys. Res.* **88,** 3273–3293 (1983).
15. Dziewonski, A. M. & Woodhouse, J. H. An experiment in systematic study of global seismicity: centroid-moment tensor solutions for 201 moderate and large earthquakes of 1981. *J. Geophys. Res.* **88,** 3247–3271 (1983).
16. Dziewonski, A. M., Ekström, G. & Maternovskaya, N.-N. Centroid-moment tensor solutions for October–December. *Phys. Earth Planet. Inter.* **115,** 1–16 (1999).
17. Abercrombie, R. E. & Mori, J. J. Local observations of the onset of a large earthquakes: 28 June 1992 Landers, California. *Bull. Seismol. Soc. Am.* **84,** 725–734 (1994).
18. Wesnousky, S. G. Seismological and structural evolution of strike-slip faults. *Nature* **335,** 340–343 (1988).
19. Harris, R. A. & Day, S. M. Dynamic 3D simulations of earthquakes on en echelon faults. *Geophys. Res. Lett.* **26,** 2089–2092 (1999).
20. Dziewonski, A. M. & Anderson, D. L. Preliminary reference Earth model. *Phys. Earth Planet. Inter.* **2,** 297–356 (1981).
21. Kanamori, H. & Anderson, D. L. Theoretical basis for some empirical relations in seismology. *Bull. Seismol. Soc. Am.* **65,** 1073–1095 (1975).
22. Chen, Y. Thermal model of oceanic transform faults. *J. Geophys. Res.* **93,** 8839–8851 (1988).
23. Detrick, R. S., White, R. S. & Purdy, G. M. Crustal structure of North Atlantic fracture zones. *Rev. Geophys.* **31,** 439–458 (1993).
24. Brune, J. N. Seismic moment, seismicity and rate of slip along major fault zones. *J. Geophys. Res.* **73,** 777–784 (1968).
25. DeMets, C., Gordon, R. G., Argus, D. F. & Stein, S. Current plate motions. *Geophys. J. Int.* **101,** 425–478 (1990).
26. Smith, W. H. F. & Sandwell, D. T. Global sea floor topography from satellite altimetry and ship depth soundings. *Science* **277,** 1956–1962 (1997).
27. Wessel, P. & Smith, W. H. F. Free software helps map and display data. *Eos* **72,** 441, 445–446 (1991).
28. Ekström, G. A very broadband inversion method for the recovery of earthquake source parameters. *Tectonophysics* **166,** 73–100 (1989).
29. Antolik, M., Kaverina, A. & Dreger, D. Compound rupture of the great 1998 Antarctic plate earthquake. *J. Geophys. Res.* **105,** 23825–23838 (2000).
30. McKenzie, D. P. Speculations on the consequences and causes of plate motions. *Geophys. J. R. Astron. Soc.* **18,** 1–32 (1969).

Acknowledgements

We thank M. Antolik for assistance with the slip inversion, and J. Tromp for discussion.

Correspondence and requests for materials should be addressed to R. E. A. (e-mail: rachel@seismology.harvard.edu).

Isotopic evidence for microbial sulphate reduction in the early Archaean era

Yanan Shen*, Roger Buick† & Donald E. Canfield*

* *Danish Center for Earth System Science (DCESS) and Institute of Biology, Odense University, SDU, Campusvej 55, 5230 Odense M, Denmark*
† *School of Geosciences FO5, University of Sydney, Sydney, NSW 2006, Australia*

Sulphate-reducing microbes affect the modern sulphur cycle, and may be quite ancient[1,2], though when they evolved is uncertain. These organisms produce sulphide while oxidizing organic matter or hydrogen with sulphate[3]. At sulphate concentrations greater than 1 mM, the sulphides are isotopically fractionated (depleted in ^{34}S) by 10–40‰ compared to the sulphate, with fractionations decreasing to near 0‰ at lower concentrations[2,4–6]. The isotope record of sedimentary sulphides shows large fractionations relative to seawater sulphate by 2.7 Gyr ago, indicating microbial sulphate reduction[7]. In older rocks, however, much smaller fractionations are of equivocal origin, possibly biogenic but also possibly volcanogenic[2,8–10]. Here we report microscopic sulphides in ~3.47-Gyr-old barites from North Pole, Australia, with maximum fractionations of 21.1‰, about a mean of 11.6‰, clearly indicating microbial sulphate reduction. Our results extend the geological record of microbial sulphate reduction back more than 750 million years, and represent direct evidence of an early specific metabolic pathway—allowing time calibration of a deep node on the tree of life.

Our samples came from the Dresser Formation (Warrawoona Group, Pilbara Craton) at North Pole in northwestern Australia. These rocks have experienced only very-low-grade metamorphism and slight deformation[11]. Their age is constrained by zircon U–Pb geochronology to 3.515–3.458 Gyr (ref. 12). The Dresser Formation consists of pillowed, amygdaloidal basalt with three interbeds of cherty metasediments. Most samples came from the lowest chert bed, from lenses of bedded barite ($BaSO_4$) within silicified volcanogenic and carbonate sediments that were deposited in a shallow